Supplementary Material for:

SWI/SNF and RSC cooperate to reposition and evict promoter nucleosomes at highly expressed genes in yeast

Supplementary Materials and Methods

Plasmid and yeast strain construction

Construction of strains carrying doxycycline repressible alleles of *STH1* were generated by replacing the *STH1* native promoter with *HIS3MX-tTA-tetO* DNA cassette. The cassette was PCR-amplified from plasmid pHQ2078 (Qiu et al. 2015) using forward primer: 5'-*CTTAAGAGGAAAAAGAGTATAGAGAAAAACAAAGGCAATCAGCGGCTAATTTGGTGGAAATAACAACA CA*CAGCTGAAGCTTCGTACGC 3' (with *STH1* promoter sequences -100 to -31 italicized) and reverse primer: 5'-*CCAATGCGGCAACTGTTGTAGGTGTATTATTCATCACCGTGCTCATCAACTCAGATTGTTCCTGAAGCAT*A TAGGCCACTAGTGGATCTG 3' (with S*TH1* CDS sequences +70 to +1 italicized), and used to transform F729 to His^+ and thereby generate P_{TET}-*STH1* strain HQY1632. The *HIS3MX-tTA-tetO* DNA cassette was alternatively recovered from plasmid pHQ2100 by StuI digestion and used to transform strain F748 to generate *snf2Δ* P_{TET}-*STH1* strain HQY1660. Replacement of the *STH1* promoter with the *HIS3MX-tTA-tetO*$_2$ cassette was confirmed by PCR analysis and Western blot analysis of Sth1 expression using antibody sc-33290 (Santa Cruz Biotechnology). Plasmid pHQ2100 was generated by inserting a 370bp *STH1* 5'UTR fragment between the HindIII-BglII sites, and a 340 bp *STH1* 5' ORF fragment (beginning with the ATG codon) between the BamHI-HpaI sites, in pHQ2078. Yeast strains with C-terminally Myc_{13}-tagged *SNF2-myc* (HQY367) or *STH1-myc* (HQY459) were previously described (Swanson et al. 2003).

MNase-ChIP-seq analysis of H3.

For MNase-ChIP-seq, yeast cells were grown, treated with SM and cross-linked with formaldehyde as described for CHIP-seq (Qiu et al. 2015), except cells were grown in 500ml cultures and harvested as 5 equal aliquots. Cells were lysed with glass beads in FA lysis buffer (50 mM Hepes-KOH [pH 7.5], 140 mM NaCl, 1 mM EDTA, 1%Triton X-100, 0.1% sodium deoxycholate, 1 mM PMSF, 1X cOmplete Protease Inhibitor Cocktail EDTA free, Roche), the chromatin-rich fraction was recovered and digested with MNase nuclease as described (Wal and Pugh 2012), with the following modifications. Each chromatin pellet was first washed with FA lysis buffer, followed by NP-S buffer (0.5 mM Spermidine, 0.075% (v/v) NP-40, 50 mM NaCl, 10 mM Tris–Cl, pH 7.5, 5 mM $MgCl_2$, 1 mM $CaCl_2$), resuspended in 0.3ml NP-S buffer with 1 mM 2-mercaptoethanol, and digested with different amounts of MNase (Worthington Biochemical, 10 U/ µL stock) for 10min at 30°C. MNase digestion was stopped by adding EDTA to 10 mM and transferring digests to ice for 10min. Digested chromatin was separated from cell debris by high speed centrifugation at 4°C, suspended in 0.3ml NP-S buffer with 0.2% SDS, and incubated 5 min before collecting by centrifugation. Both supernatants were combined and saved as MNase-digested chromatin; and 100µL aliquots were adjusted to 200µL with NP-S buffer and examined for input analysis as described previously (Qiu et al. 2015) for sonicated chromatin. For each yeast strain, MNase digestion giving 70-80% mononucleosomes were selected for immunoprecipitation, as follows. Aliquots containing 5.0µg of DNA were adjusted to 500µL using NP-S buffer and 1X FA lysis buffer from 4X stock and mixed with 2µg anti-H3 antibodies (Abcam) conjugated with anti-rabbit dynabeads and immunoprecipitated overnight. Immune complexes were washed and treated to reverse cross-linking, DNA was precipitated, and

paired-end libraries were prepared and sequenced as described previously (Qiu et al. 2015) for ChIP-seq of sonicated samples.

Estimation of the positions of +1/-1 nucleosomes

To determine the median positions of +1 and -1 nucleosomes for each gene and all strains, we first used the MNase-ChIP-seq data and the method described in (Qiu et al. 2015) to identify the typical positions of these nucleosomes. Those values were then refined using the following algorithm. For each position of +1/-1 nucleosomes identified using the method described in Qiu et al. 2015, we used a symmetrical window of 147 bp and computed all nucleosome dyad positions that were mapped by MNase-ChIP-seq in this window and the corresponding median position. This position was used as an estimation of the median nucleosome position in a population of cells. The estimated positons of +1/-1 nucleosomes, NDR center and NDR width for uninduced and induced WT and examined mutants are listed in Table S3.

Estimation of typical inter-nucleosomal spacing

To estimate the typical nucleosome spacing, for each gene we first used k-means clustering to identify the 5 clusters of MNase-ChIP-seq reads corresponding to nucleosomes +1, +2, +3, +4, +5, using the *kmeans* function in MATLAB. Then we performed a linear regression using the positions of all read centers belonging to the 5 clusters, using the *fitlm* function in MATLAB, and the regression coefficient (the slope of the fitted line) that we obtained was used to estimate the typical inter-nucleosomal spacing for each yeast gene.

Identification of nucleosomes not evicted from NDRs in the *P_{TET}-STH1 snf2Δ* mutant

An iterative algorithm was used to identify nucleosomes located within NDRs of the of the *P_{TET}-STH1 snf2Δ* strain but absent in WT. For each gene, we first tiled the whole NDR with overlapping windows of 147bp shifted by 50bp from each other. Then we computed the locations of the MNase-ChIP-seq read centers found in each window, and the corresponding median position of the reads. Each window was then shifted to be centered at the median position and the procedure was repeated until all of the median positions of the reads were at most 1bp apart from the center of the corresponding window (i.e. until all window shifts that were needed for the next iteration were ≤ 1 bp). The centers of the final windows indicate the median positions for the clusters of nucleosome dyads corresponding to nucleosomes that occupy similar positions in a population of cells, i.e. typical positions of the nucleosomes in the *P_{TET}-STH1 snf2Δ* double mutant. Out of these positions, we filtered and retained the positions where the nucleosome occupancy was ≤ 0.25 in the WT strain, and ≥ 0.4 in the double mutant. Then we manually inspected the gene promoters that were depleted in WT cells but occupied by nucleosomes in *P_{TET}-STH1 snf2Δ* cells, and split these into the 3 groups shown in Fig. 6D.

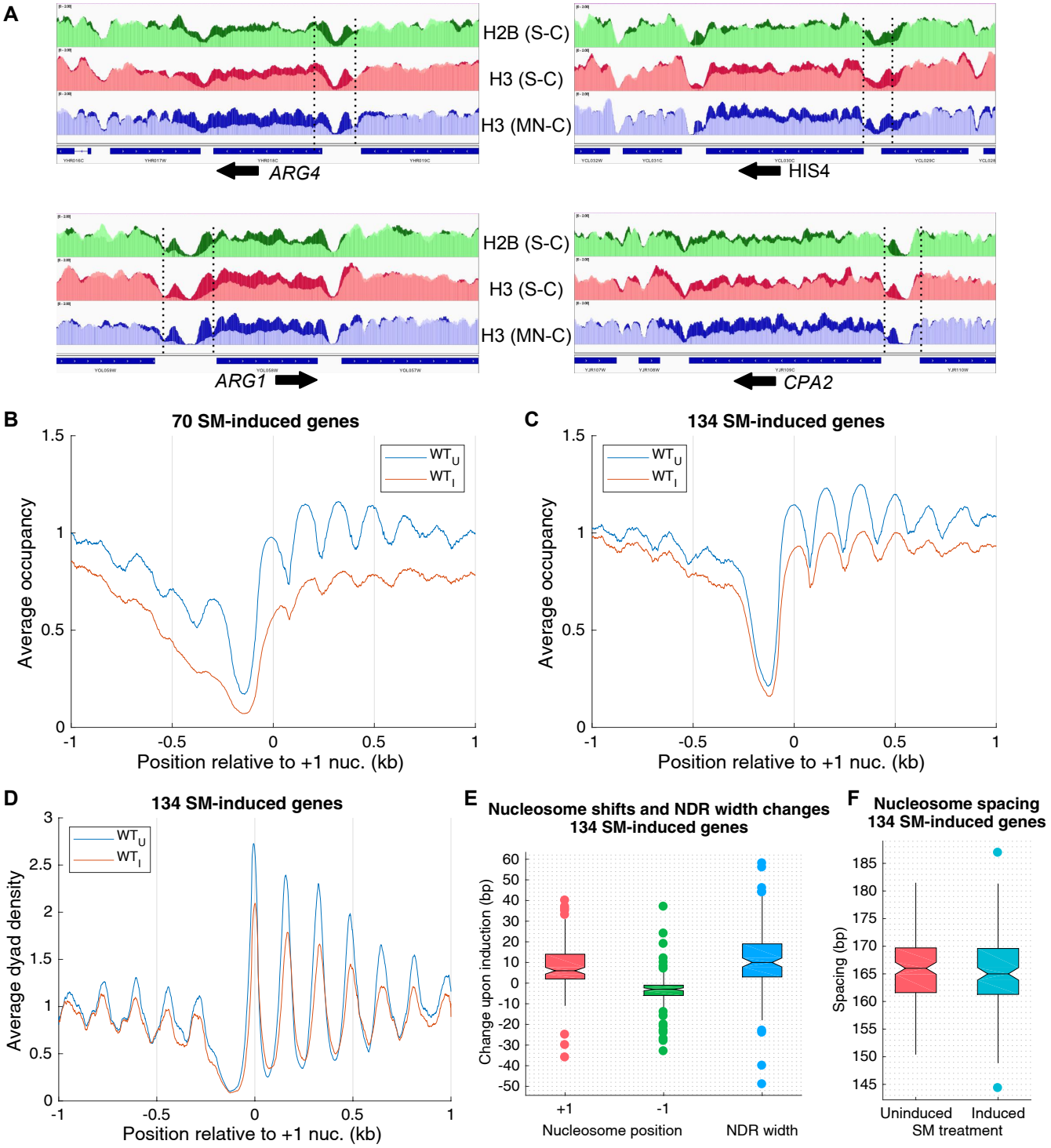
A
H2B (S-C)
H3 (S-C)
H3 (MN-C)
ARG4
HIS4
ARG1
CPA2
B
70 SM-induced genes
WT_U
WT_I
Average occupancy
Position relative to +1 nuc. (kb)
C
134 SM-induced genes
D
134 SM-induced genes
Average dyad density
E
Nucleosome shifts and NDR width changes
134 SM-induced genes
Change upon induction (bp)
+1
-1
Nucleosome position
NDR width
F
Nucleosome spacing
134 SM-induced genes
Spacing (bp)
Uninduced
Induced
SM treatment

Figure S1. **Supporting evidence for eviction and sliding of promoter nucleosomes at SM-induced genes in WT cells.** (A) IGV profiles of histone H2B and H3 occupancies from ChIP-seq with sonicated chromatin (S-C) (50-150 bp reads), and H3 occupancies from MNase-ChIP-seq (MN-C) (50-200 bp reads), for canonical Gcn4 target genes *ARG1, ARG4, HIS4* and *CPA2*, before (darker colors) and after (lighter colors) SM treatment. (B, C) Plots of normalized and averaged H3 occupancies at each base pair aligned to the +1 nucleosome calculated from MNase-ChIP-seq data for the 70 exemplar SM-induced genes (B), or for the remaining 134 less-remodeled SM-induced genes (C). Blue and red profiles, results from uninduced and SM-induced WT cultures, respectively. (D) Average dyad densities aligned to the +1_Nuc for the 134 SM-induced genes, depicted as in Fig. 1E. Average profiles were smoothed using a moving average filter with a span of 31 bp. (E) Boxplots depicting shifts in +1 and -1 nucleosome positions, and changes in NDR widths, for the 134 SM-induced genes, analyzed as in Fig. 1F. (F) Boxplots depicting nucleosome spacing for the array of +1 to +5 nucleosomes, for the 134 SM-induced genes in uninduced and SM-induced WT cells, as in Fig. 1G.

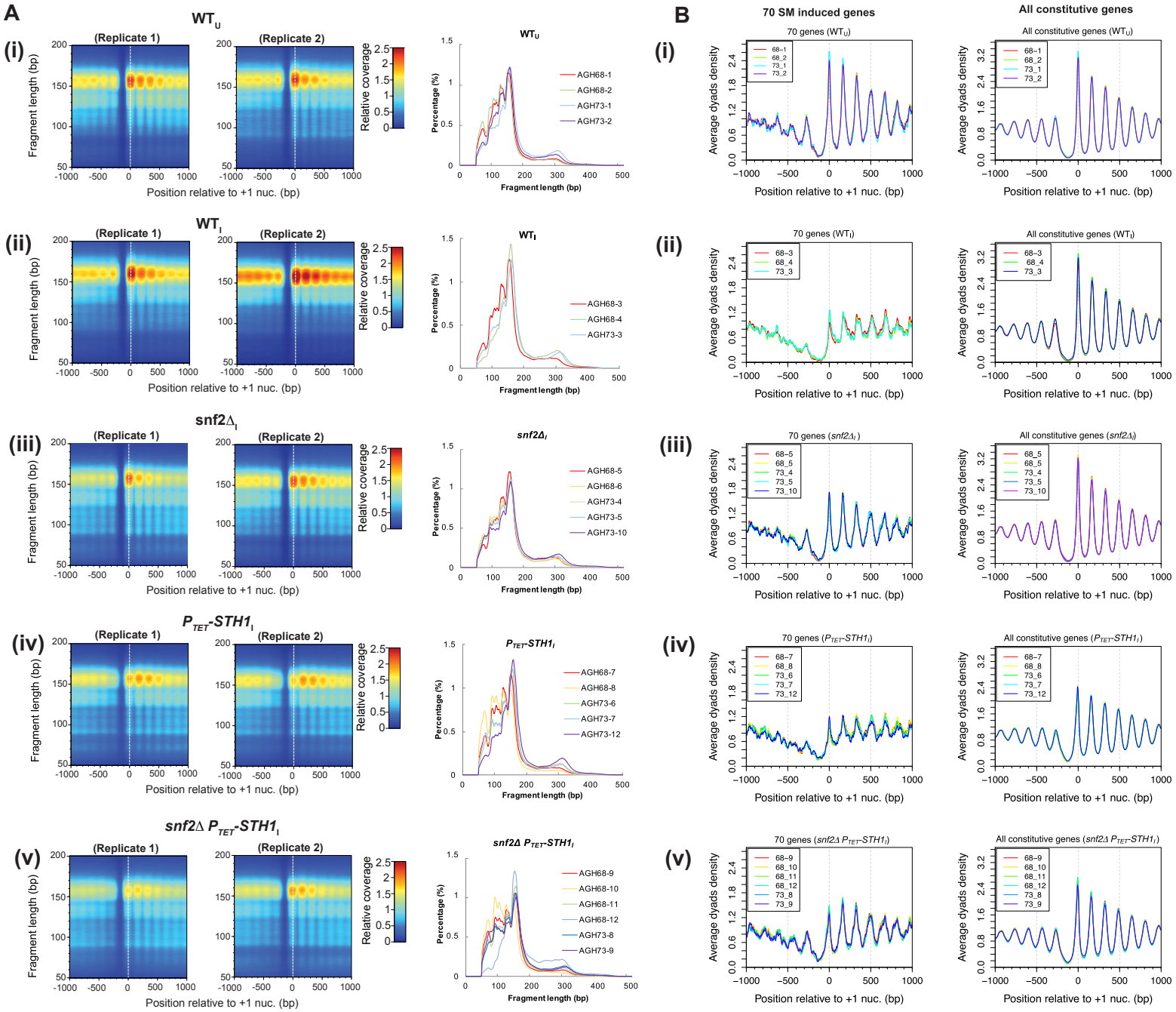
A
WT_U
(i)
(Replicate 1)
(Replicate 2)
Fragment length (bp)
Position relative to +1 nuc. (bp)
Relative coverage
Percentage (%)
Fragment length (bp)
AGH68-1
AGH68-2
AGH73-1
AGH73-2
WT_I
(ii)
AGH68-3
AGH68-4
AGH73-3
snf2Δ_I
(iii)
AGH68-5
AGH68-6
AGH73-4
AGH73-5
AGH73-10
P_TET-STH1_I
(iv)
AGH68-7
AGH68-8
AGH73-6
AGH73-7
AGH73-12
snf2Δ P_TET-STH1_I
(v)
AGH68-9
AGH68-10
AGH68-11
AGH68-12
AGH73-8
AGH73-9
B
70 SM induced genes
All constitutive genes
(i)
70 genes (WT_U)
All constitutive genes (WT_U)
68–1
68_2
73_1
73_2
(ii)
70 genes (WT_I)
All constitutive genes (WT_I)
68–3
68_4
73_3
(iii)
70 genes (snf2Δ_I)
All constitutive genes (snf2Δ_I)
68–5
68_5
73_4
73_5
73_10
(iv)
70 genes (P_TET-STH1_I)
All constitutive genes (P_TET-STH1_I)
68–7
68_8
73_6
73_7
73_12
(v)
70 genes (snf2Δ P_TET-STH1_I)
All constitutive genes (snf2Δ P_TET-STH1_I)
68–9
68_10
68_11
68_12
73_8
73_9
Average dyads density
Position relative to +1 nuc. (bp)

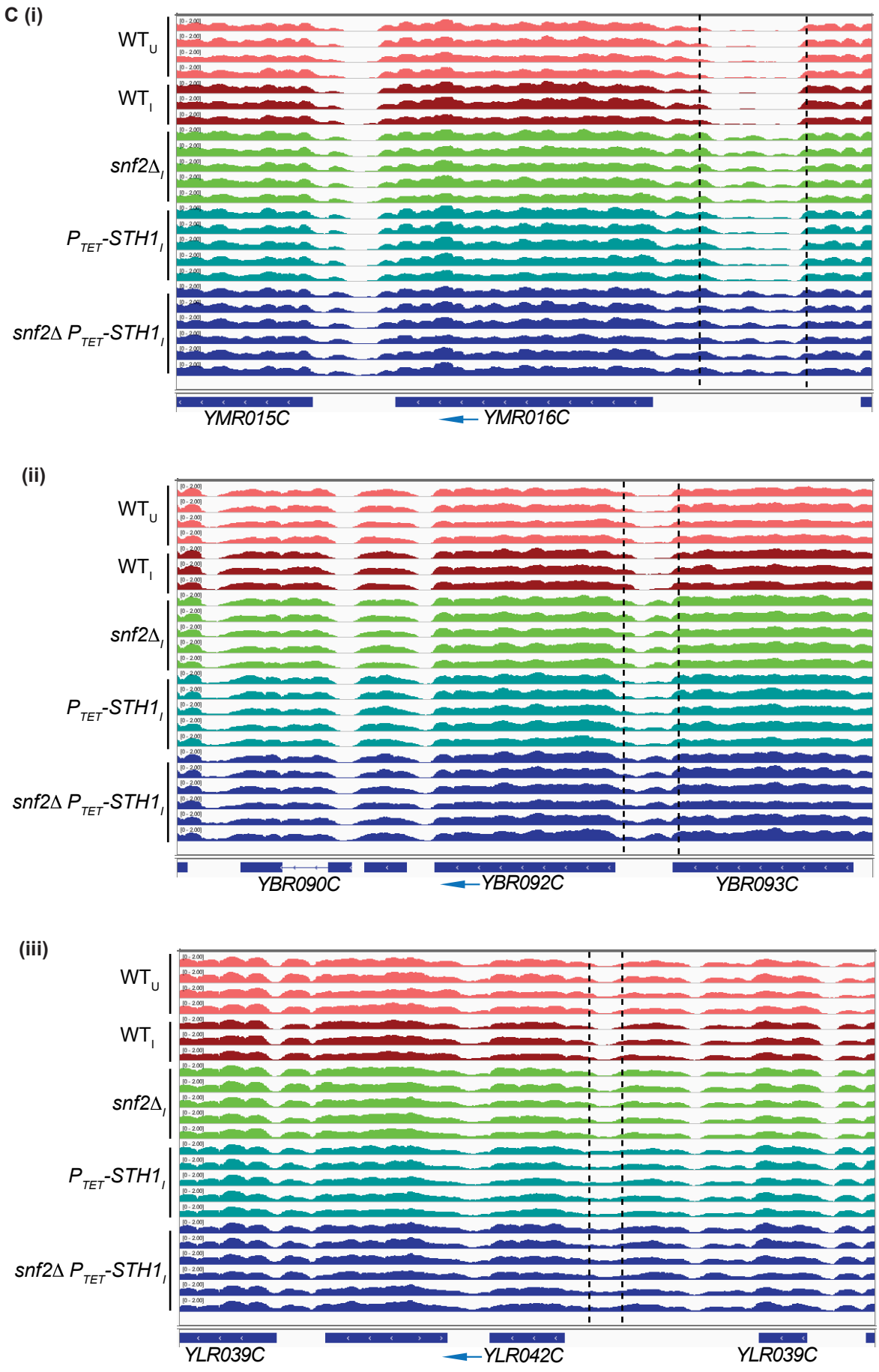
C (i)
WT U
WT I
snf2Δ I
P TET-STH1 I
snf2Δ P TET-STH1 I
YMR015C
YMR016C
(ii)
WT U
WT I
snf2Δ I
P TET-STH1 I
snf2Δ P TET-STH1 I
YBR090C
YBR092C
YBR093C
(iii)
WT U
WT I
snf2Δ I
P TET-STH1 I
snf2Δ P TET-STH1 I
YLR039C
YLR042C
YLR039C

Figure S2. **Variations in fragment length distributions in replicates of H3 MNase-ChIP-seq experiments do not affect determinations of average nucleosome dyad positions or nucleosome occupancies for the groups of 70 SM-induced genes or all constitutive genes.** (A) 2D occupancy plots (see Chereji et al. 2017 and https://github.com/rchereji/plot2DO) indicating the relative coverage of the MNase-ChIP-seq fragments of different lengths (50-200 bp), in 2 kb regions centered on the +1 nucleosome dyads of all yeast genes. The X axis indicates the position relative to the +1 nucleosome dyad, the Y axis indicates DNA fragment length, and the color at position (*x, y*) represents the relative coverage obtained by stacking all the DNA fragments of length *y* that covered position *x*. Red indicates high coverage, while dark blue indicates zero coverage. Two biological replicates are shown for uninduced or SM-induced WT (i, ii), or the indicated mutants under inducing conditions (iii-v). On the right, the histogram of MNase-ChIP-seq fragment lengths (i.e. percentages of total reads for each fragment length) are plotted for all biological replicates for each strain/condition depicted on the left. (B) Average nucleosome dyad densities in 2 kb regions centered on the typical positions of the +1 nucleosomes for the group of 70 SM-induced genes (left column) and all constitutive genes (right column), calculated as in Fig. 1E for each biological replicate of MNase-ChIP-seq data obtained for the five indicated strains/conditions analyzed in this study. Average dyad density plots shown in all other figures were calculated after pooling the reads from all replicates for each strain. (C) IGV profiles of histone H3 occupancies from MNaset ChIPt seq of three genes, analyzed in Fig. 5B, calculated from each biological replicate of the five indicated strains/conditions analyzed in this study.

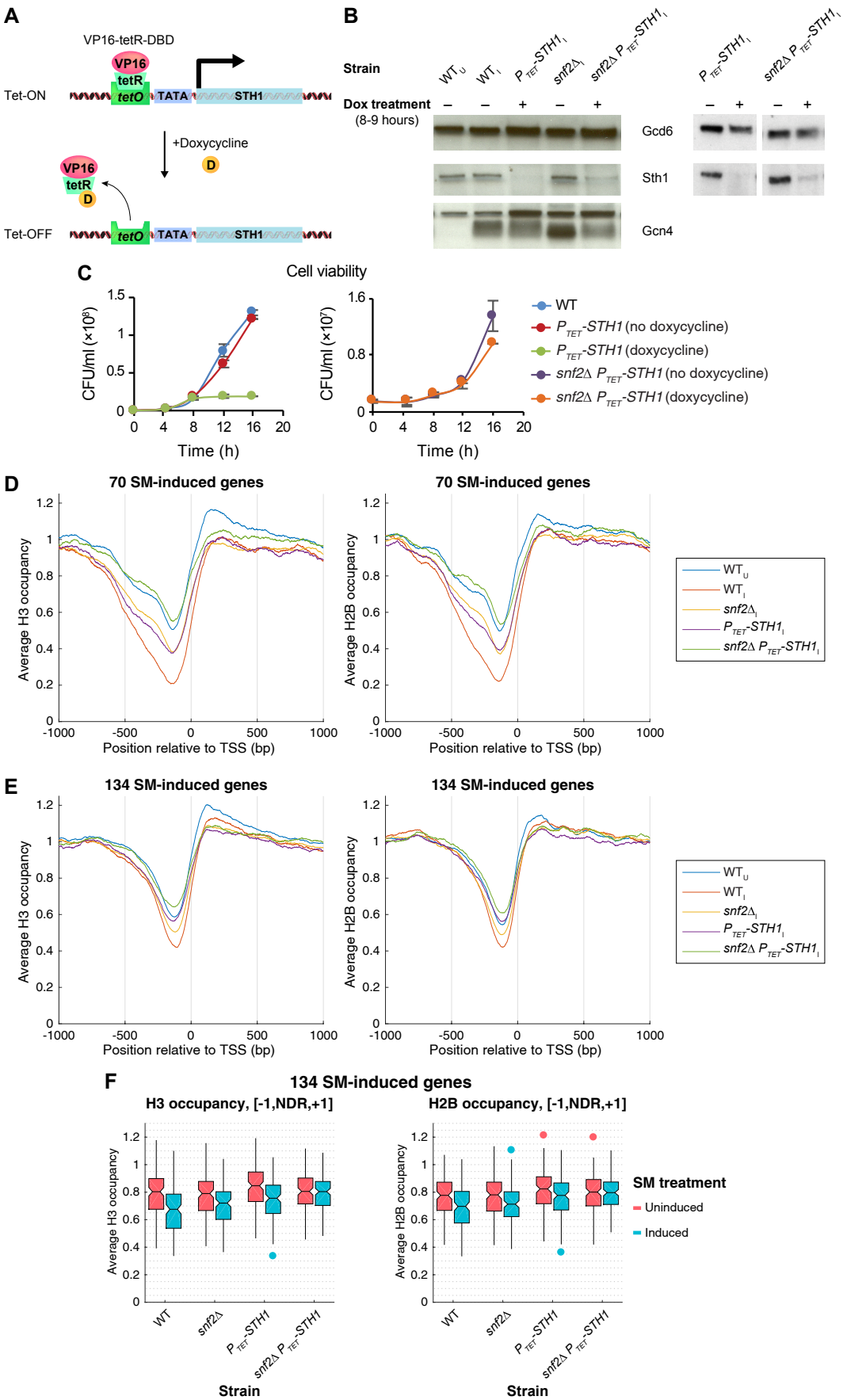
A
VP16-tetR-DBD
VP16
tetR
tetO
TATA
STH1
Tet-ON
+Doxycycline
D
Tet-OFF
B
Strain
Dox treatment
(8-9 hours)
Gcd6
Sth1
Gcn4
C
Cell viability
CFU/ml (×10^8)
CFU/ml (×10^7)
Time (h)
WT
P_TET-STH1 (no doxycycline)
P_TET-STH1 (doxycycline)
snf2Δ P_TET-STH1 (no doxycycline)
snf2Δ P_TET-STH1 (doxycycline)
D
70 SM-induced genes
Average H3 occupancy
Average H2B occupancy
Position relative to TSS (bp)
E
134 SM-induced genes
F
H3 occupancy, [-1,NDR,+1]
H2B occupancy, [-1,NDR,+1]
SM treatment
Uninduced
Induced
Strain

Figure S3. **Supporting evidence for defects in eviction of promoter nucleosomes at SM-induced genes in the three remodeler mutants.** (A) Diagram depicting regulation of *STH1* transcription from the tetracycline-repressible promoter. Binding of tetracycline analog doxycycline to the VP16-tetR-DBD activator protein, expressed from the promoter cassette, releases it from the *tetO* operator, turning off transcription of the P_{TET}-*STH1* allele. (B) Western analysis of whole cell extracts of strains of the indicated genotype cultured in SC-ILV medium and treated (+) or left untreated (-) with 10 μg/ml doxycycline for 8-9h, using antibodies against Gcd6 (loading control), Sth1 or Gcn4. For induced samples (lanes 2-5), cells were treated with SM for 25 min as for ChIP-seq analysis. (C) Strains of indicated genotypes were cultured in SC-ILV medium with 10 μg/ml doxycycline or no doxycycline, from an initial A_{600} of 0.075, and cell viability was estimated by plating dilutions of culture aliquots, collected at 4h intervals, on YPD agar plates and calculating colony forming units (CFU) per ml. As eliminating *SNF2* decreases vegetative growth, the effect of depleting Sth1 is shown separately in *SNF2* and *snf2Δ* cells (*right;* note difference in y-axis scale). No decrease in CFU was observed between 8-16h incubation in the presence of doxycycline. (D, E) Plots of averaged H3 or H2B occupancies at each base pair aligned to the TSS calculated from ChIP-seq data for (D) 70 or (E) 134 SM-induced genes for the indicated yeast strains, as in Fig. 1 A. (F) Notched box plots of H2B or H3 occupancies per nucleotide in the [−1,NDR,+1] regions calculated from ChIP-seq data from at least three replicates of the indicated yeast strains for the group of 134 SM-induced.

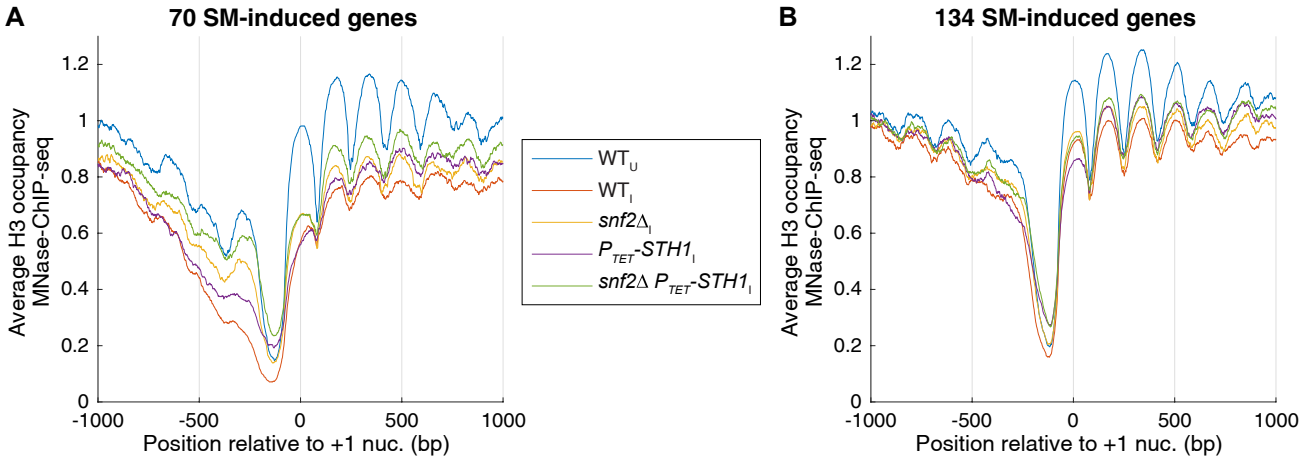
A
70 SM-induced genes
Average H3 occupancy
MNase-ChIP-seq
1.2
1
0.8
0.6
0.4
0.2
0
-1000
-500
0
500
1000
Position relative to +1 nuc. (bp)
WT_U
WT_I
snf2Δ_I
P_TET-STH1_I
snf2Δ P_TET-STH1_I
B
134 SM-induced genes
Average H3 occupancy
MNase-ChIP-seq
Position relative to +1 nuc. (bp)

Figure S4. Additional supporting evidence for defects in nucleosome eviction at SM-induced genes in the remodeler mutants. (A, B) Plots of averaged H3 occupancies at each base pair aligned to the +1 nucleosome calculated from H3 MNase-ChIP-seq data for the groups of (A) 70 and (B) 134 SM-induced genes for the indicated strains. For each gene, reads were normalized to the average occupancy on the respective chromosome.

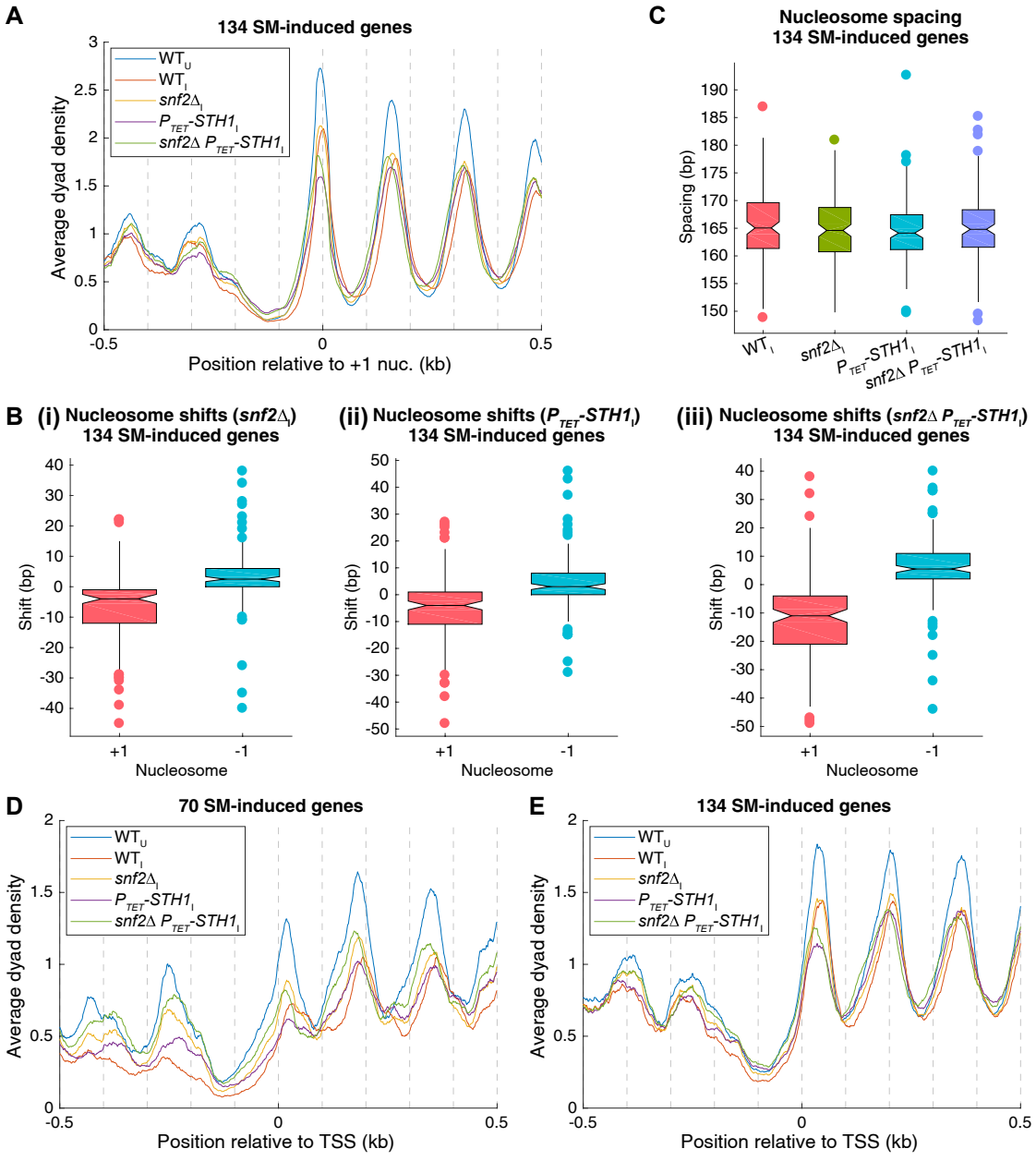
A
134 SM-induced genes
Average dyad density
Position relative to +1 nuc. (kb)
WT_U
WT_I
snf2Δ_I
P_TET-STH1_I
snf2Δ P_TET-STH1_I
C
Nucleosome spacing
134 SM-induced genes
Spacing (bp)
B
(i) Nucleosome shifts (snf2Δ_I)
134 SM-induced genes
(ii) Nucleosome shifts (P_TET-STH1_I)
134 SM-induced genes
(iii) Nucleosome shifts (snf2Δ P_TET-STH1_I)
134 SM-induced genes
Shift (bp)
Nucleosome
+1
-1
D
70 SM-induced genes
Position relative to TSS (kb)
E
134 SM-induced genes
Position relative to TSS (kb)

Figure S5. Supporting evidence for defects in re-positioning of promoter nucleosomes at SM-induced genes in the three remodeler mutants. (A) Average dyad density plot aligned to the +1 nucleosome for 134 SM-induced genes for the indicated yeast strains, calculated as in Fig. 1E. (B-C) Boxplots depicting change in +1 and -1 nucleosome positions (B) or nucleosome spacing (C) for the 134 SM-induced genes in the indicated remodeler mutants under inducing conditions versus WT_I cells, determined as in Figs. 1F-G. (D-E) Average dyad densities aligned to the TSS were calculated from MNase-ChIP-seq as in Fig. 1E for the (D) 70 and 134 (E) SM-induced genes in the indicated yeast strains. All average dyad profiles were smoothed using a moving average filter with a span of 31 bp.

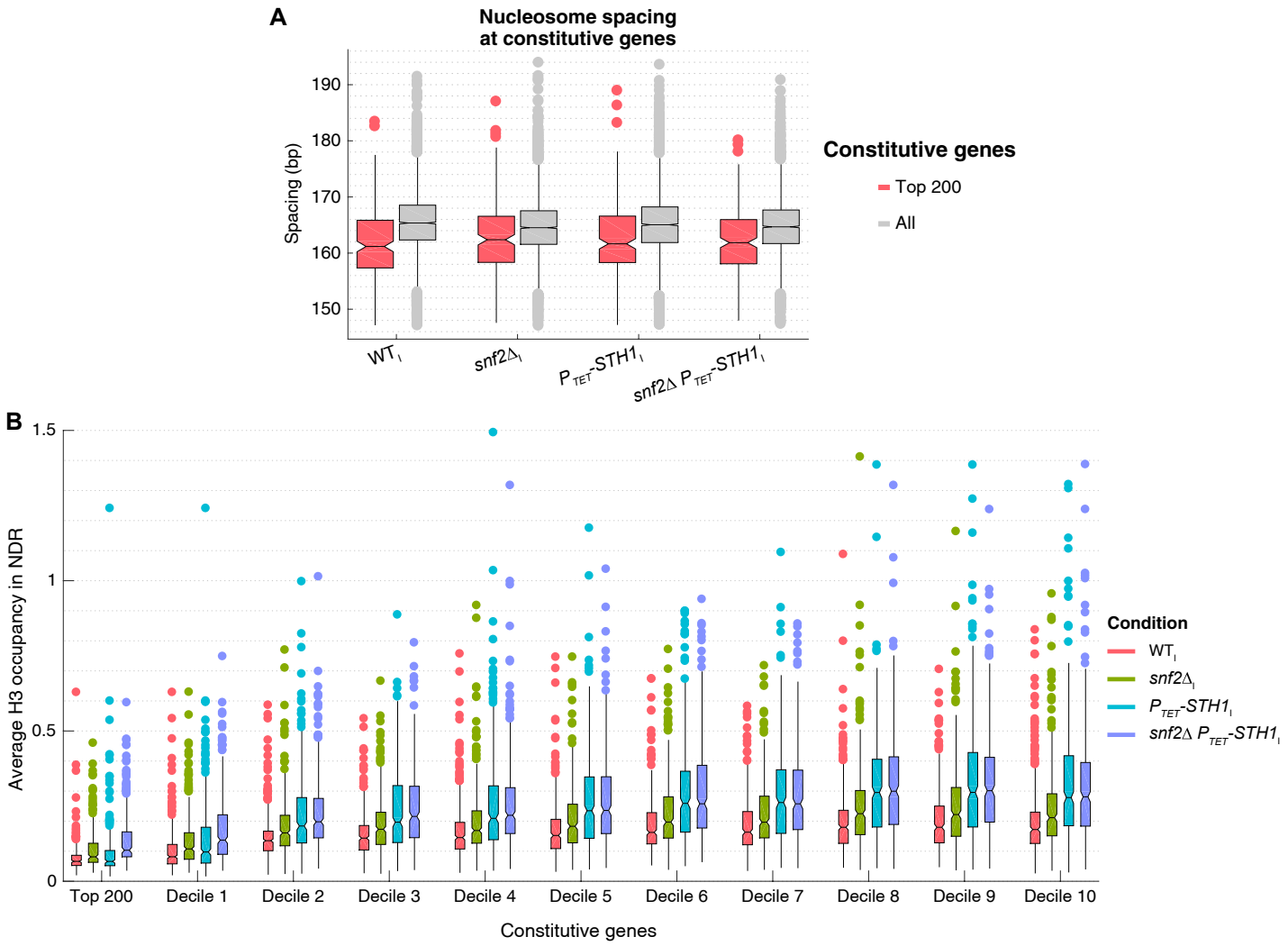
A
Nucleosome spacing
at constitutive genes
Spacing (bp)
190
180
170
160
150
WT_I
snf2Δ_I
P_TET-STH1_I
snf2Δ P_TET-STH1_I
Constitutive genes
Top 200
All
B
Average H3 occupancy in NDR
1.5
1
0.5
0
Top 200
Decile 1
Decile 2
Decile 3
Decile 4
Decile 5
Decile 6
Decile 7
Decile 8
Decile 9
Decile 10
Constitutive genes
Condition
WT_I
snf2Δ_I
P_TET-STH1_I
snf2Δ P_TET-STH1_I

Figure S6. Supporting evidence for defects in clearing nucleosomes from NDRs in the remodeler mutants at only the most highly expressed subset of constitutive genes. (A) Boxplots depicting nucleosome spacing in indicated strains, calculated from H3 MNase-ChIP-seq data for all 3619 constitutive genes (grey) or the Top 200 expressed constitutive genes (red). (B) Notched box plots of H3 occupancies per nucleotide in NDRs calculated from H3 MNase-ChIP-seq data for the indicated strains, for deciles of 3619 constitutive genes sorted by Rpb3 occupancies as in Fig. 3C.

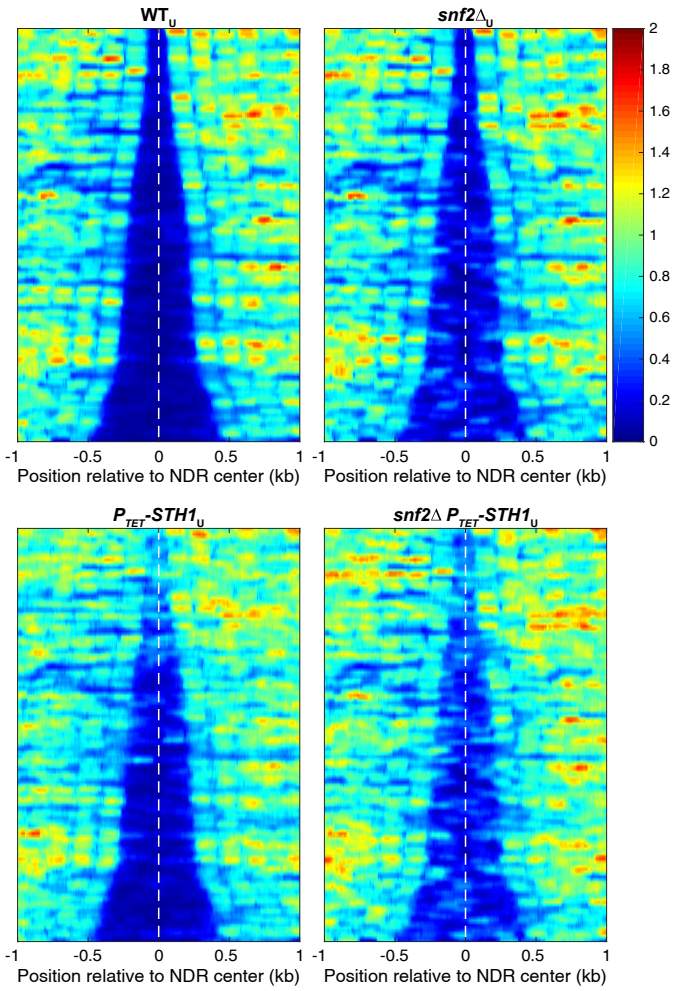
WT_U
snf2Δ_U
P_TET-STH1_U
snf2Δ P_TET-STH1_U
2
1.8
1.6
1.4
1.2
1
0.8
0.6
0.4
0.2
0
-1
-0.5
0
0.5
1
Position relative to NDR center (kb)

Figure S7. Appearance of new nucleosome peaks in the NDRs of certain constitutively expressed genes in the *snf2Δ* P_{TET}*-STH1* double mutant under non-inducing conditions. Heat map depictions of H3 occupancies calculated from MNase-ChIP-seq data of the indicated yeast strains for a group of 162 genes selected from among all genes that exhibit nucleosome peaks in *snf2Δ* P_{TET}*-STH1* cells not evident in WT cells, aligned to NDR centers; sorting genes by NDR width uninduced WT cells, and color-coded as shown on right.

Table S1. Yeast strains used in this study

Strain Name	Parent	Genotype	Source
F729/ BY4741	NA	*MATa his3Δ1 leu2Δ0 met15Δ0 ura3Δ0*	Research genetics
F748	BY4741	*MATa his3Δ1 leu2Δ0 met15Δ0 ura3Δ0 snf2Δ::kanMX4*	Research genetics
HQ1632	BY4741	*MATa his3Δ1 leu2Δ0 met15Δ0 ura3Δ0 HIS3MX6::P_{TET}-STH1*	This study
HQ1660	F748	*MATa his3Δ1 leu2Δ0 met15Δ0 ura3Δ0 snf2Δ::kanMX4 HIS3MX6::P_{TET}-STH1*	This study
HQY367	BY4741	*MATa his3Δ1 leu2Δ0 met15Δ0 ura3Δ0 SNF2-myc_{13}::HIS3MX6*	Swanson et al., 2003
HQY459	BY4741	*MATa his3Δ1 leu2Δ0 met15Δ0 ura3Δ0 STH1-myc_{13}::HIS3MX6*	Swanson et al., 2003

Table S2. ChIP-seq replicates

Sonication H3/ChIP-seq

Genotype	Sample ID	SM	Dox	All PE reads	rmdup PE reads	Source
WT_U	AGH58_02	−	-	29625671	8011769	This study
WT_U	AGH62_01	−	-	14993257	8597216	This study
WT_U	AGH62_02	−	-	19032734	9965205	This study
$snf2\Delta_U$	AGH57_4	−	−	23934378	15075565	This study
$snf2\Delta_U$	AGH57_5	−	−	24825347	15914213	This study
$snf2\Delta_U$	AGH57_6	−	−	26587486	16214184	This study
P_{TET}-$STH1_U$	AGH57_7	−	+	23796469	14253969	This study
P_{TET}-$STH1_U$	AGH57_8	−	+	25699355	16305759	This study
P_{TET}-$STH1_U$	AGH57_9	−	+	22301447	13116189	This study
$snf2\Delta$ P_{TET}-$STH1_U$	AGH57_10	−	+	28571112	15491126	This study
$snf2\Delta$ P_{TET}-$STH1_U$	AGH57_11	−	+	26364759	17057518	This study
$snf2\Delta$ P_{TET}-$STH1_U$	AGH57_12	−	+	24518529	15058743	This study
WT_I	AGH58_04	+	-	20620578	5466934	This study
WT_I	AGH62_03	+	-	18617080	8200524	This study
WT_I	AGH62_08	+	-	19798491	5044590	This study
$snf2\Delta_I$	AGH59_01	+	-	14174694	7052399	This study
$snf2\Delta_I$	AGH59_02	+	-	14573693	6456125	This study
$snf2\Delta_I$	AGH62_05	+	-	20877009	10613818	This study
$snf2\Delta_I$	AGH04_01	+	-	15597956	11985536	Qiu et al., 2015
$snf2\Delta_I$	AGH04_02	+	-	17071372	13099928	Qiu et al., 2015
$snf2\Delta_I$	AGH25_01	+	-	24839200	11548218	Qiu et al., 2015
P_{TET}-$STH1_I$	AGH50_01	+	+	23176098	12629620	This study
P_{TET}-$STH1_I$	AGH54_03	+	+	22858502	9011007	This study
P_{TET}-$STH1_I$	AGH50_06	+	+	26443231	6284621	This study
$snf2\Delta$ P_{TET}-$STH1_I$	AGH54_01	+	+	23674356	12035478	This study
$snf2\Delta$ P_{TET}-$STH1_I$	AGH54_02	+	+	27937517	13179773	This study
$snf2\Delta$ P_{TET}-$STH1_I$	AGH50_10	+	+	30027139	5408247	This study

Table S2. ChIP-seq replicates

Sonication H2B/ChIP-seq

Genotype	Sample ID	SM	Dox	All PE reads	rmdup PE reads	Source
WT_U	AGH60_02	−	−	19628438	8322922	This study
WT_U	AGH45_01	−	−	12208679	7927728	This study
WT_U	AGH45_02	−	−	11961060	7894189	This study
$snf2\Delta_U$	AGH67_4	−	−	16534315	9227553	This study
$snf2\Delta_U$	AGH67_5	−	−	15540476	9198843	This study
$snf2\Delta_U$	AGH67_6	−	−	17857046	9504690	This study
P_{TET}-$STH1_U$	AGH67_7	−	+	15288646	7792881	This study
P_{TET}-$STH1_U$	AGH67_8	−	+	15109854	7489350	This study
P_{TET}-$STH1_U$	AGH67_9	−	+	15934988	7644091	This study
$snf2\Delta$ P_{TET}-$STH1_U$	AGH67_10	−	+	19450474	9425352	This study
$snf2\Delta$ P_{TET}-$STH1_U$	AGH67_11	−	+	19924639	10652912	This study
$snf2\Delta$ P_{TET}-$STH1_U$	AGH67_12	−	+	16494713	8657324	This study
WT_I	AGH60_04	+	−	21838062	15319809	This study
WT_I	AGH45_03	+	−	11376591	8144250	This study
WT_I	AGH62_11	+	−	20225185	3857138	This study
$snf2\Delta_I$	AGH60_11	+	−	19367826	13137056	This study
$snf2\Delta_I$	AGH60_12	+	−	19010109	12759019	This study
$snf2\Delta_I$	AGH45_10	+	−	14370641	9342565	This study
$snf2\Delta_I$	AGH48_07	+	−	28893689	12565519	This study
$snf2\Delta_I$	AGH48_08	+	−	27731080	10801903	This study
$snf2\Delta_I$	AGH48_09	+	−	26318644	10449013	This study
P_{TET}-$STH1_I$	AGH63_04	+	+	22504481	8826667	This study
P_{TET}-$STH1_I$	AGH63_05	+	+	21296504	8101558	This study
P_{TET}-$STH1_I$	AGH63_06	+	+	21746584	6489767	This study
$snf2\Delta$ P_{TET}-$STH1_I$	AGH63_07	+	+	24234763	10877407	This study
$snf2\Delta$ P_{TET}-$STH1_I$	AGH63_08	+	+	22770272	10101318	This study
$snf2\Delta$ P_{TET}-$STH1_I$	AGH63_09	+	+	21969413	10797105	This study

Table S2. ChIP-seq replicates

Sonication Rpb3/ChIP-seq

Genotype	Sample ID	SM	Dox	All PE reads	rmdup PE reads	Source
WT_U	AGH03_1	−	−	12103981	7624104	Qiu et al., 2015
WT_U	AGH03_2	−	−	15621065	10271685	Qiu et al., 2015
WT_U	AGH03_3	−	−	14624526	8895936	Qiu et al., 2015
WT_I	AGH03_4	+	−	10978154	7859118	Qiu et al., 2015
WT_I	AGH03_5	+	−	16862702	11526037	Qiu et al., 2015
WT_I	AGH03_6	+	−	14660604	10042576	Qiu et al., 2015
$snf2\Delta_I$	AGH12_7	+	−	14213867	10131580	Qiu et al., 2015
$snf2\Delta_I$	AGH12_8	+	−	12857958	8200570	Qiu et al., 2015
$snf2\Delta_I$	AGH28_1	+	−	13651250	1859651	Qiu et al., 2015
P_{TET}-$STH1_I$	AGH51_01	+	+	6836169	1768416	This study
P_{TET}-$STH1_I$	AGH51_05	+	+	12990191	2395951	This study
P_{TET}-$STH1_I$	AGH51_06	+	+	13376423	2103356	This study
$snf2\Delta$ P_{TET}-$STH1_I$	AGH51_02	+	+	12853198	1909934	This study
$snf2\Delta$ P_{TET}-$STH1_I$	AGH51_09	+	+	11798395	1996785	This study
$snf2\Delta$ P_{TET}-$STH1_I$	AGH51_10	+	+	12653664	2171622	This study

Table S2. ChIP-seq replicates

MNase H3/ChIP-seq

Genotype	Sample ID	SM	Dox	All PE reads	rmdup PE reads	Source
WT_U	AGH68_01	−	−	21155789	16387173	This study
WT_U	AGH68_02	−	−	29890860	21290074	This study
WT_U	AGH73_01	−	−	22748400	13752475	This study
WT_U	AGH73_02	−	−	33931620	20843860	This study
WT_I	AGH68_03	+	−	22985503	17204691	This study
WT_I	AGH68_04	+	−	19959153	15376225	This study
WT_I	AGH73_03	+	−	26493831	17942518	This study
$snf2\Delta_I$	AGH68_05	+	−	20896164	15789365	This study
$snf2\Delta_I$	AGH68_06	+	−	23587865	18055776	This study
$snf2\Delta_I$	AGH73_04	+	−	30193725	20155496	This study
$snf2\Delta_I$	AGH73_05	+	−	28834376	19622426	This study
$snf2\Delta_I$	AGH73_10	+	−	27351420	18319655	This study
P_{TET}-$STH1_I$	AGH68_07	+	+	21614150	16939365	This study
P_{TET}-$STH1_I$	AGH68_08	+	+	24081014	18755148	This study
P_{TET}-$STH1_I$	AGH73_06	+	+	29619041	19719008	This study
P_{TET}-$STH1_I$	AGH73_07	+	+	26053659	18067975	This study
P_{TET}-$STH1_I$	AGH73_12	+	+	24618600	16927985	This study
$snf2\Delta$ P_{TET}-$STH1_I$	AGH68_09	+	+	24352916	18823892	This study
$snf2\Delta$ P_{TET}-$STH1_I$	AGH68_10	+	+	35625027	24578682	This study
$snf2\Delta$ P_{TET}-$STH1_I$	AGH68_11	+	+	26104427	19584798	This study
$snf2\Delta$ P_{TET}-$STH1_I$	AGH68_12	+	+	19106755	11875757	This study
$snf2\Delta$ P_{TET}-$STH1_I$	AGH73_08	+	+	27010389	18495503	This study
$snf2\Delta$ P_{TET}-$STH1_I$	AGH73_09	+	+	25011131	17657515	This study
$snf2\Delta_U$	AGH81_02	−	−	26607113	15776809	This study
$snf2\Delta_U$	AGH81_03	−	−	20857397	12924899	This study
$snf2\Delta_U$	AGH87_01	−	−	22806847	16781714	This study
$snf2\Delta_U$	AGH87_02	−	−	30330091	19522950	This study
P_{TET}-$STH1_U$	AGH81_04	−	+	20916061	9659542	This study
P_{TET}-$STH1_U$	AGH81_06	−	+	26818025	15411529	This study
$snf2\Delta$ P_{TET}-$STH1_U$	AGH81_07	−	+	22293847	9415935	This study
$snf2\Delta$ P_{TET}-$STH1_U$	AGH81_08	−	+	21967556	10049178	This study
$snf2\Delta$ P_{TET}-$STH1_U$	AGH87_03	−	+	19552427	13629844	This study

snf2Δ P_{TET}-STH1$_U$	AGH87_04	−	+	22712961	15551050	This study
snf2Δ P_{TET}-STH1$_U$	AGH87_09	−	+	16429859	11194834	This study
snf2Δ P_{TET}-STH1$_U$	AGH87_10	−	+	25099770	16500031	This study